

Supporting Information

Ion-Specific Assembly of Strong, Tough, and Stiff Biofibers

Nitesh Mittal⁺, Tobias Benselfelt⁺,* Farhan Ansari, Korneliya Gordeyeva, Stephan V. Roth, Lars Wågberg, and L. Daniel Söderberg**

anie_201910603_sm_miscellaneous_information.pdf

Experimental Section

CNFs Preparation and Characterization. Carboxymethylated CNF gels (solid weight content ~1 wt.%) were provided by RISE Bioeconomy (Stockholm) with a carboxylate content of 0.6 mmol/g. CNF dispersions were prepared by diluting the gels with DI water using a similar protocol described by us earlier.^[1] Chemically bleached softwood pulp (with an average mixture of 60% Norwegian spruce and 40% Scots pine, Domsjo AB, Sweden) were used as a starting material for the preparation of the fibrils. Length and height of nanofibrils were measured using transmission electron microscopy and atomic force microscopy, respectively, by using a protocol described elsewhere.^[2] The average length and height of nanofibrils were 686 ± 250 nm and 2–3 nm, respectively (Figures S1 and S2).

Film Preparation. CNF films were prepared by vacuum filtration using Durapore hydrophilic PVDF filters with pore sizes of 0.65 μm according to an earlier described procedure.^[3] A 0.2 wt % CNF dispersion was filtered over night to produce a filter cake with a diameter of 8 mm and a solids content of 5-10 wt%. The filter cakes were dried in the drying section of a Rapid-Köthen sheet former (Paper Testing Instruments, Austria) for 20 min at 50 or 93 °C and a reduced pressure of 95 kPa. The films were soaked in acid of pH 2 before or after the initial drying.

Microfluidic Setup and Fiber Preparation. The microfluidic setup consists of a double flow-focusing channel geometry, three syringe pumps (WPI, AI-4000), and a DI water bath (Figure S3). The three syringe pumps supply (1) CNFs dispersion in the core flow, (2) DI water in the first

sheath, and (3) gel initiator in the second sheath flows of the channel. Flow rates of the core and sheath flows were set to 4.1, 4.4, and 24.6 mL h⁻¹, respectively. The channel was milled into stainless-steel plate (1 mm thickness) and sealed between plexiglas plates on both sides. Aluminum plates were placed on either side and screwed together to prevent the leakage. The width of channels was 1 mm. The outlet of the channel was submerged in a DI water bath. CNF hydrogel threads were picked up from the water bath with the help of tweezers followed by drying in the air at room temperature (23°C) for at least 2 h. Solid CNF fibers were obtained after drying.

Fiber Characterization. Scanning electron microscope (SEM) samples were prepared by sputtering the fibers surface with a 5 nm thin gold–palladium layer (Gressington Instruments Ltd., UK). Surface morphology of fibers was detected by using a field emission scanning electron microscope (Hitachi S-4800, Japan) operated at an acceleration voltage of 1 keV.

WAXS measurements were done at PETRA III storage ring (P03 beamline) at DESY, Hamburg.^[4] Three samples for each case were measured. Measurements were performed at an X-ray wavelength $\lambda = 0.96 \text{ \AA}$, with a sample-to-detector distance of 71 mm. Size of the beam was $6 \times 14 \text{ \mu m}^2$ (horizontal \times vertical). Scattering diffractograms were recorded using a Pilatus 300-k detector (Dectris) with a pixel size of $172 \times 172 \text{ \mu m}^2$. Orientation index (f_c), was calculated as per the below equation^[1]

$$f_c = \frac{180^\circ - fwhm}{180^\circ}$$

where $fwhm$ is the full width at half-maximum (indicated by red arrows in Figure S5).

Tensile Test Measurements. Tensile tests of fibers were performed with a Universal Materials Testing Machine from Instron (E100) equipped with a 5 N load cell using a similar protocol to that

reported elsewhere.^[2] Fibers were conditioned at room temperature (23°C) and 50% RH for at least a day prior to testing. The dimensions were measured by an optical microscope (Nikon Japan-Eclipse Ni-E) and further crosschecked with SEM for a few samples. Individual CNF fibers were uniform in cross section throughout the length; however, the diameter may differ between the different fibers. Typical diameters of the dried CNF fibers were around $7.0 \pm 1.5 \mu\text{m}$. The gauge length was 8–12 mm, and measurements were carried out at a crosshead speed of 0.5 mm min^{-1} . The cross section of the fibers was assumed to be circular based on the SEM analysis. At least 10 different measurements for each type of biofiber sample were conducted.

Tensile test of films were performed with an Instron 5944 equipped with a 500 N load cell using a similar protocol to that reported elsewhere.^[5] Films were conditioned at room temperature (23°C) and 50% RH for at least a day prior to testing. The dimensions were measured with a caliper and typical dimensions were a thickness of $50 \mu\text{m}$ and a width of 3 mm. The gauge length was 20 mm and measurements were carried out at a crosshead speed of 2 mm min^{-1} . At least 4 different measurements for each type of film sample were conducted.

The analysis of the tensile data (strength, toughness and stiffness) was done using MATLAB. Toughness is defined as work to fracture and was defined as the area under stress-strain curve.^[6] Modulus was determined from the initial linear regime.^[2]

Elemental analysis. Elemental analysis was used to measure the actual amount of different ions inside the fibers. Sulfur content was measured using CHNS-O analysis using flash combustion and gas chromatography (Thermo FlashEA 1112). Chlorine content was determined by oxygen flask combustion and subsequent titration with mercuric nitrate. Iron and phosphorous contents were determined by acid digestion and subsequent analysis using inductively coupled plasma optical

spectroscopy (ICP-OES, varian Vista MPX CCD). A minimum of 5 mg fibers were used for each analysis which was performed in duplicates. The analysis was carried out by MEDAC Ltd. in UK.

FTIR. Fourier transformed infrared spectroscopy was used to measure the state of the carboxylic acids in dried fibers and films. A Perkin-Elmer Spectrometer 100 with a Graseby Specac LTD Golden attenuated total reflectance (ATR) gate was used under ambient conditions.

Rheology. Rheology measurements of CNFs hydrogels were carried out at room temperature (23°C) using a DHR-2 rheometer (TA Instruments, USA) equipped with a Peltier plate for temperature control and a 25 mm diameter parallel plate setup with a truncation gap of 500 µm. After placing 400 µL of dispersion between the parallel plates, 0.3 mL of gel initiator (either acids or FeCl₃ solution) were added along the circumference to attain gelation (Figure 4a). Subsequently, 0.25% strain was applied, and measurements of storage and loss modulus were carried out for a period of 1 hour (until the time a constant measurement value was reached). After that, fracture stress was measured with increasing strain from 0.01% to 100% at a constant frequency of 1 Hz.

Based on the different network properties, anisotropic hydrogels should behave different than the isotropic hydrogels we used in the rheology measurements. The effect of different anions is likely to be greater if it was possible to run rheology with anisotropic hydrogels that better represents the oriented gel threads.

Water content measurements. Anisotropic hydrogels were prepared by adding the gel initiator at pH 2 (200 mL) on top of a 0.3 wt% CNF dispersion (50 mL in a 250 mL beaker) and allow it to cure for 2 hours. Excess acid was removed and the hydrogels were rinsed in 100 mL DI water for 1 hour and subsequently dried at 60 °C until “completely” dry (4 days). Pieces with a weight of

30-60 mg were weighed in the dry state, placed at 50% relative humidity for 2 days, and the mass change due to moisture sorption was measured.

Ion Chromatography. Presence of ions in the CNF films was detected using Ion Chromatography (Metrohm 761 Compact Ion Chromatograph, Switzerland) by using a similar protocol to that described elsewhere.^[7] In this method, ions were extracted from solid films using deionized water. In brief, a suppressed conductivity detector was used to detect the specific anions with a scale of $250 \mu\text{S cm}^{-1}$. The instrument is being optimized with respect to the maximum signal-to-noise ratio. 20 μL injection volume was used per sample for every analysis. Metrohm data acquisition system was used for the collection of data. The analysis was carried out by MEDAC Ltd. in UK.

Statistical analysis. Error bars are presented as 90 or 95 % confidence intervals based on a t-distribution.

SUPPLEMENTARY FIGURES

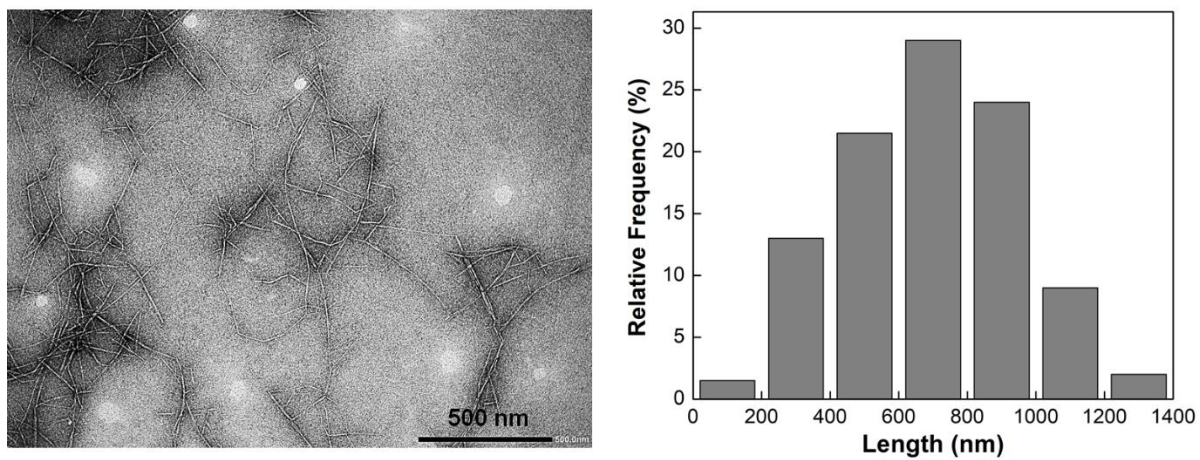


Figure S1. TEM image and length distribution of CNFs calculated from TEM images. Black spots are due to the staining of CNFs.

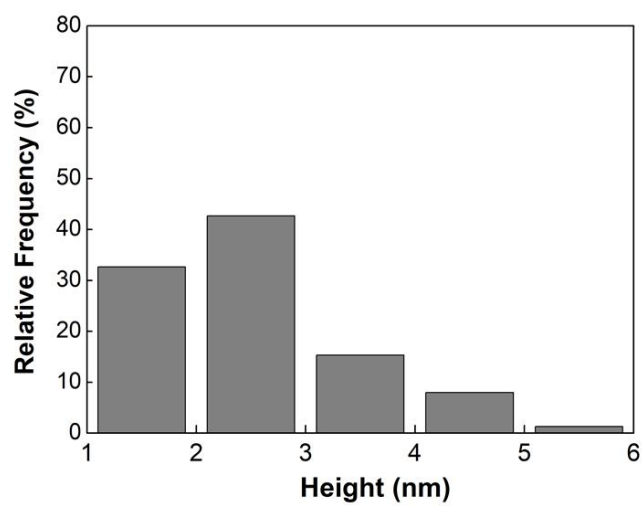
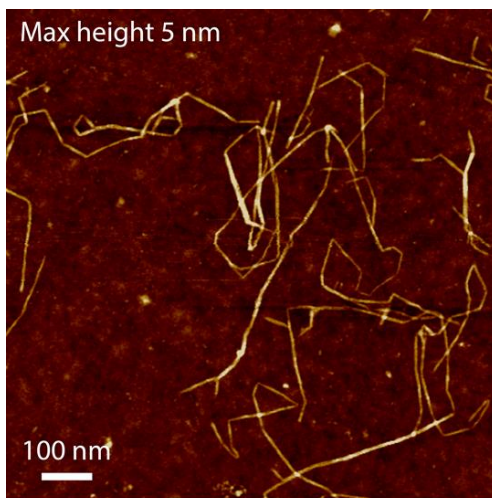


Figure S2. AFM image and height distribution of CNFs measured from AFM images.

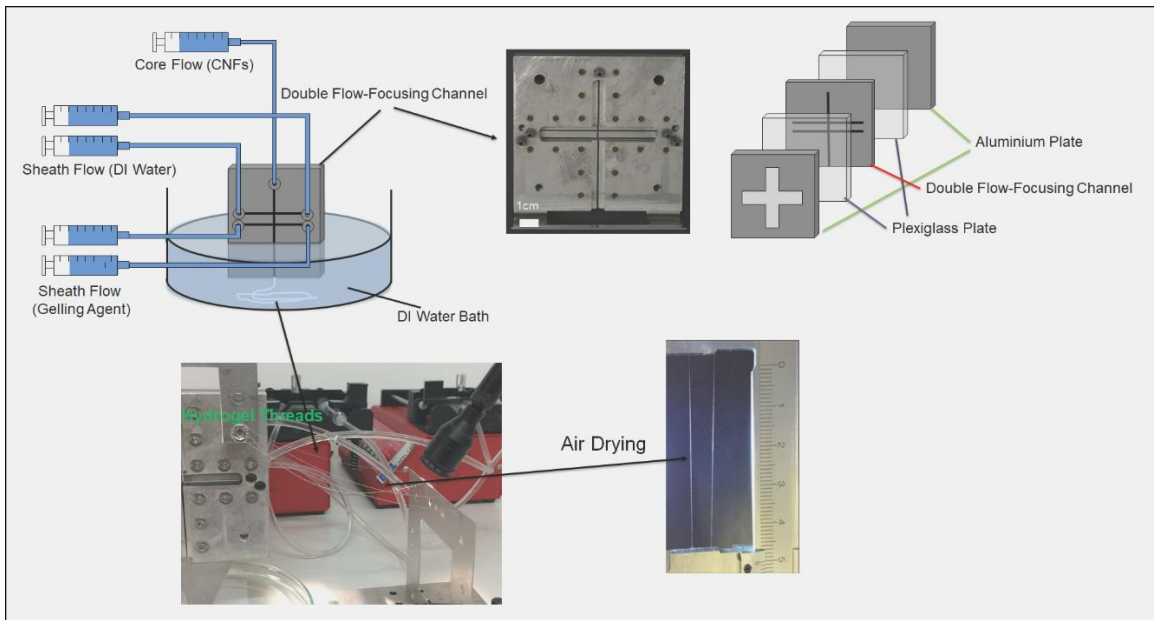


Figure S3. Schematic of the experimental setup used to assemble CNFs into macrofibres. It consists of three syringe pumps, a double flow-focusing channel, and a DI water bath to collect the hydrogel threads.

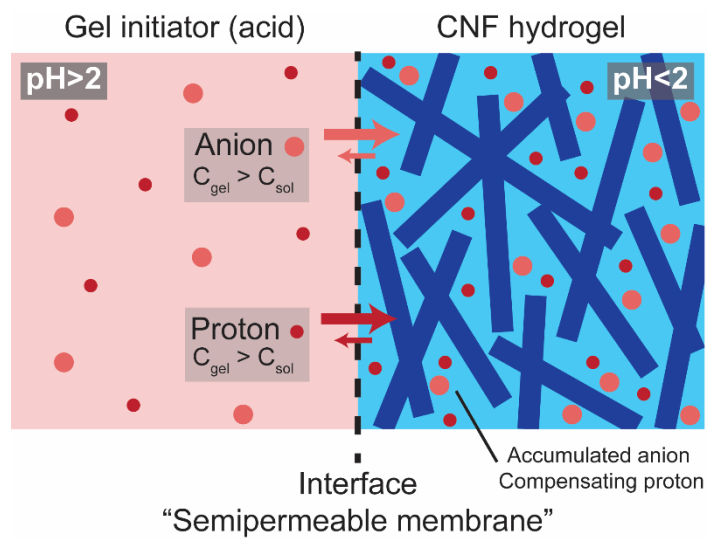


Figure S4. Schematic of the theory of local pH inside the CNF hydrogel, which is determined by the accumulation of chaotropic anions close to chaotropic CNF surfaces and the immediate balancing of charges by protons.

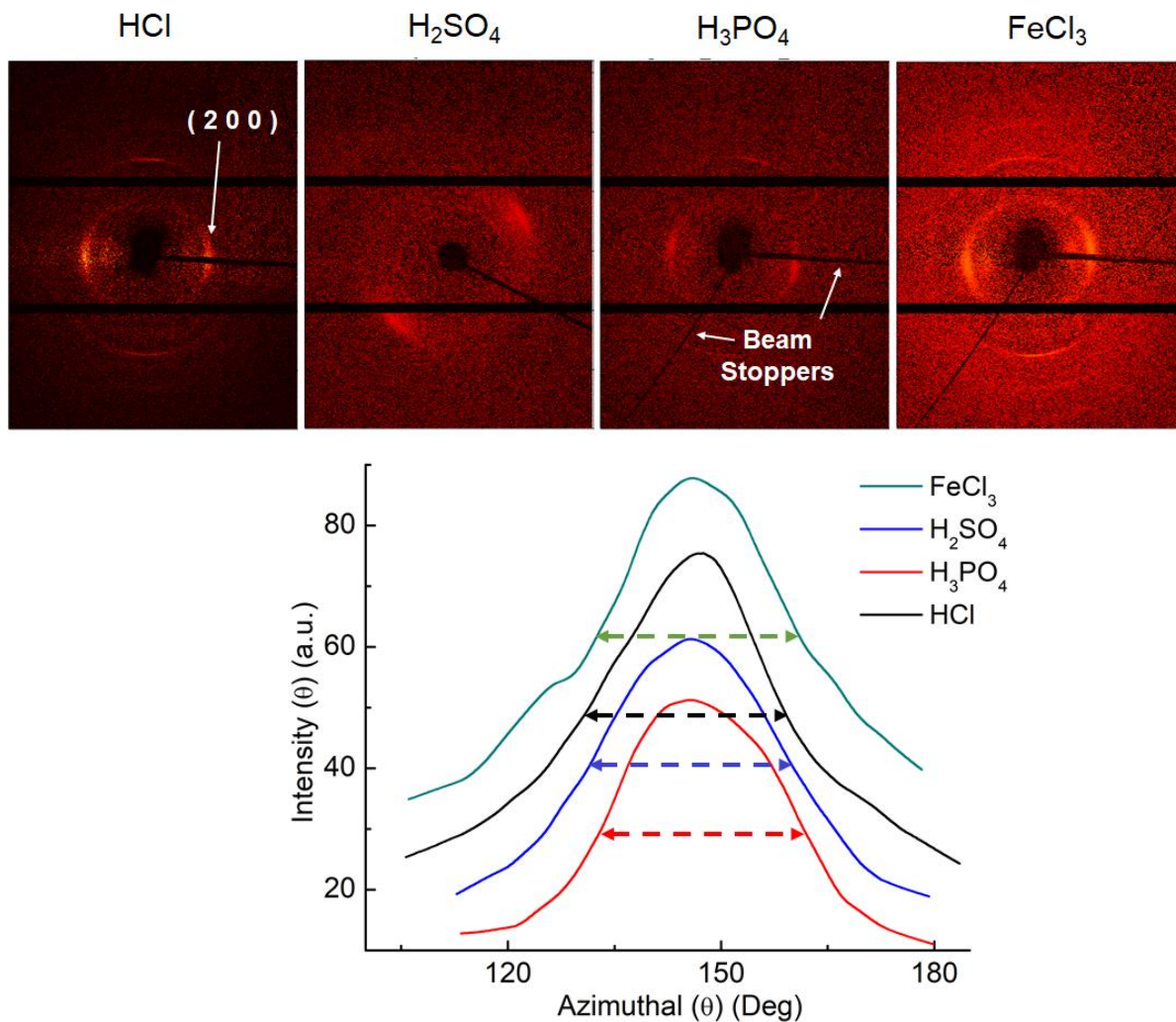


Figure S5. WAXS diffractograms of CNF fibers prepared using different gelling agents (HCl, H₂SO₄, H₃PO₄ and FeCl₃) on top. Below is the azimuthal integration of (200) scattering plane.

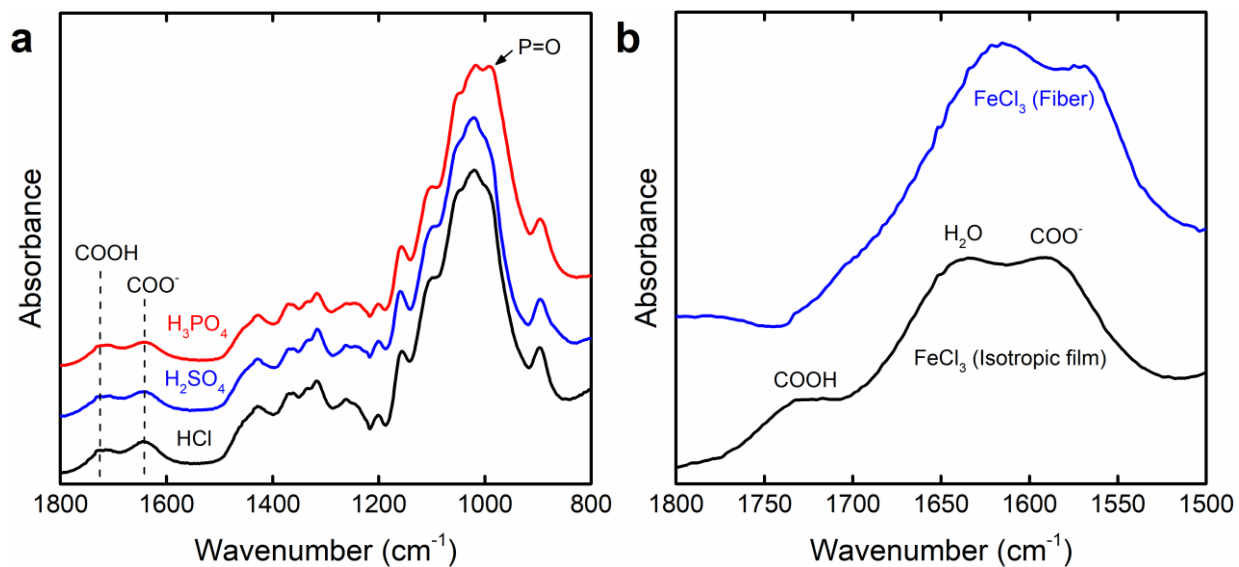


Figure S6. FTIR data for fibers prepared from 0.3 wt.% dispersions at pH 2. a) Fingerprint region of fibers prepared using sulfuric, phosphoric and hydrochloric acids. b) Carbonyl vibrations of an iron chloride treated oriented fiber and isotropic film. In a), indication of P=O vibrations is observed, but indications of sulfates are overlapping with vibrations associated with CNFs.

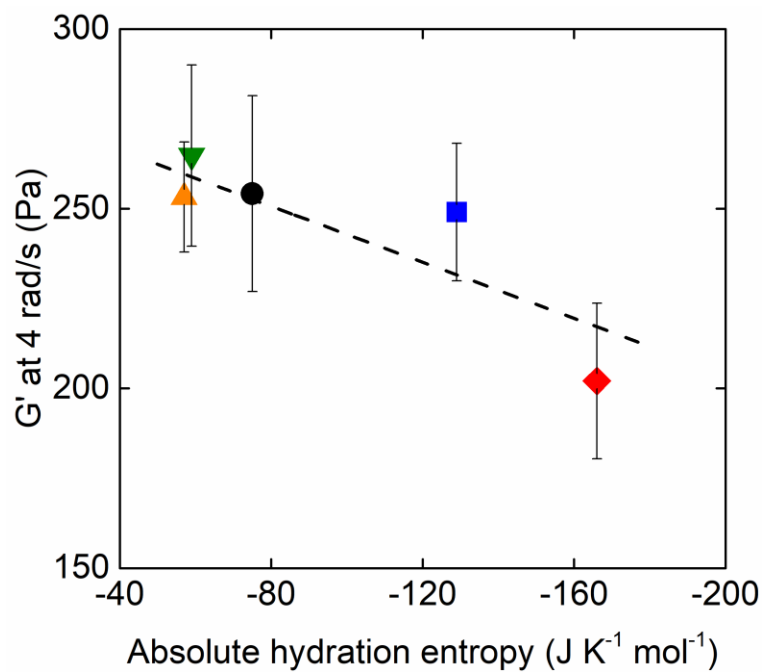


Figure S7. Relationship between the storage modulus of the CNF hydrogels and the hydration entropy of the anion.^[8] Colors and shapes are according to Figure 4.

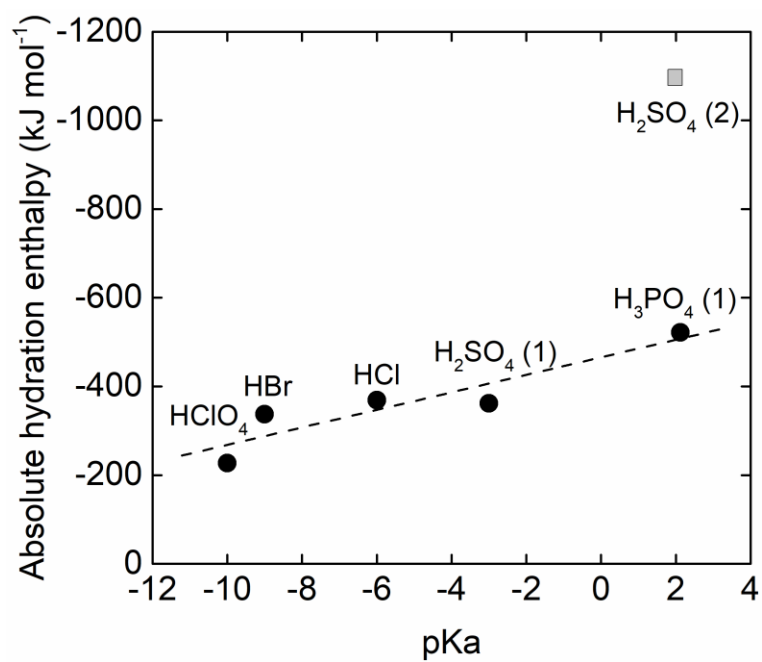


Figure S8. Relationship between hydration enthalpy and pKa of the different acids.

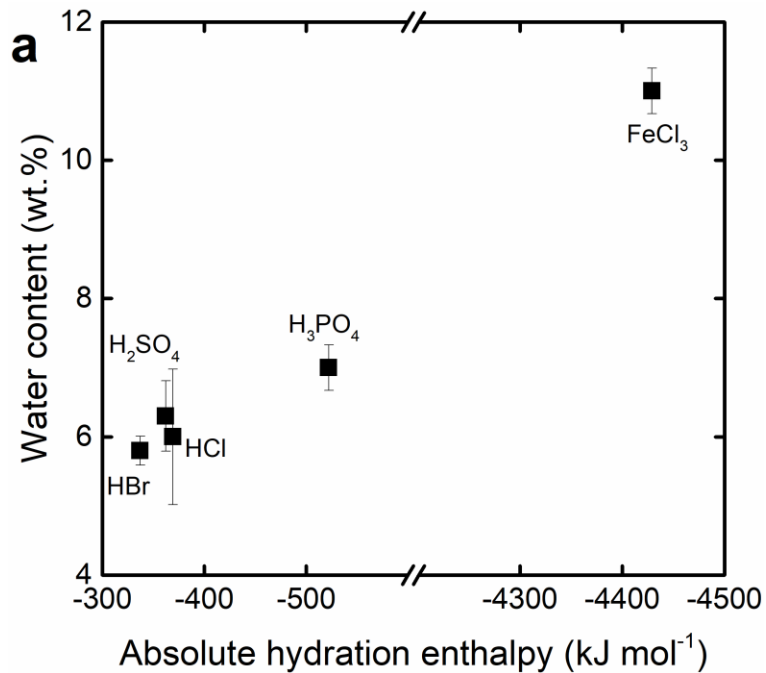


Figure S9. Water content, due to moisture sorption (50% relative humidity) into extensively dried hydrogels, as a function of the hydration enthalpy of the anions or cations in the gel initiation solution. Error bars are standard deviations ($n=3$).

SUPPLEMENTARY TABLES

Table S1. Comparison of the mechanical properties of our CNF fibres with the cellulose based fibres reported in the literature.

Cellulose Fiber/Material Type	Strength (MPa)	Stiffness (GPa)	Reference
Viscose	340	10.8	Adusumali <i>et al.</i> ^[9]
Modal	437	13.2	Adusumali <i>et al.</i> ^[9]
Lyocell	790	30.5	Adusumali <i>et al.</i> ^[9]
Rayon	778	22.2	Adusumali <i>et al.</i> ^[9]
Flax	904	40.0	Adusumali <i>et al.</i> ^[9]
CNF	535	14.5	Gao <i>et al.</i> ^[10]
CNF	150	20.0	Mohammadi <i>et al.</i> ^[11]
CNF	306	15.3	Mertaniemi <i>et al.</i> ^[12]
CNF	321	23.6	Iwamoto <i>et al.</i> ^[13]
CNF	222	12.6	Hooshmand <i>et al.</i> ^[14]
CNF	275	22.5	Walther <i>et al.</i> ^[15]
CNF	323	37.7	Rendon <i>et al.</i> ^[16]
CNF	576	18.8	Håkansson <i>et al.</i> ^[17]
CNF	297	21.0	Lundahl <i>et al.</i> ^[18]
CNF	850	53.5	Mittal <i>et al.</i> ^{[1]*}
CNF	1570	86.0	Mittal <i>et al.</i> ^{[2]*}
CNF	1010	57.0	Present Work

*These are the references of our previous studies on the mechanical properties of CNF and CNF-silk composite fibers prepared using double flow-focusing channel. Results highlight that CNF fibers prepared using double flow-focusing channel have superior tensile properties compared to the cellulose fibers prepared with other approaches. The mechanical properties in the present study are lower than the properties reported in our previous study (Reference 2) as CNFs are not covalently cross-linked as is the case in our previous study. Moreover, our previous study (Reference 2) had been done using the lab-made nanofibrils, whereas commercial CNFs from RISE Bioeconomy are used in the present work.

Table S2. Elemental analysis of fibers prepared from 0.3 wt.% dispersions at pH 2.

	Sample 1 % wt./wt.	Sample 2 % wt./wt.	Average % wt./wt.	molar mass	% mol/wt.	conc. at pH 2 (M)	content in fiber content in solution
Cl	1.47	1.64	1.56	35.453	0.044	0.01	4,4
S	0.89	0.91	0.9	32.065	0.028	0.0066	4,3
P	2.39	3.03	2.71	30.974	0.088	0.0235	3,7
Fe	8.99	8.4	8.695	55.845	0.156	n/a	n/a

The content in fiber divided by the content in solution (marked grey) is a measure (arbitrary unit) of how large a portion of the available molecules enters the fibers during the manufacturing. For phosphate this portion is lower than for Cl and S.

Table S3. Moisture sorption at 50 % relative humidity of extensively dried hydrogels at 60 °C. The hydrogels were prepared from a 0.3 wt% CNF dispersion and different gel initiators at pH 2.

	Water content at 50% RH (%)	Standard deviation (n=3)	Hydration enthalpy of the anion (kJ mol⁻¹)	Young's modulus of biofibers (GPa)
HBr	5.8	0.21	-337	
HCl	6	0.98	-369	57
H ₂ SO ₄	6.3	0.51	-362	47
H ₃ PO ₄	7	0.33	-522	36
FeCl ₃	11	0.33	-4429	39

Table S4. Comparison of the mechanical properties of the isotropic CNF films in Figure 5. The data is given as the average of at least 4 different measurements \pm 95% confidence intervals.

Sample	Strength (MPa)	Stiffness (GPa)	Strain at break (%)
HCl (dry-acid-dry)	263 \pm 14	10.0 \pm 0.2	9.6 \pm 1.4
HBr (dry-acid-dry)	243 \pm 18	10.0 \pm 0.5	7.7 \pm 1.0
H ₂ SO ₄ (dry-acid-dry)	259 \pm 9	9.8 \pm 0.2	10.0 \pm 1.4
H ₃ PO ₄ (dry-acid-dry)	257 \pm 21	9.8 \pm 0.2	9.7 \pm 2.0
HClO ₄ (dry-acid-dry)	266 \pm 4	10.2 \pm 0.3	9.3 \pm 0.8
HCl (acid-dry)	249 \pm 17	9.3 \pm 0.3	10.4 \pm 1.7
HBr (acid-dry)	244 \pm 13	9.0 \pm 0.4	10.0 \pm 1.0
H ₂ SO ₄ (acid-dry)	237 \pm 9	9.2 \pm 0.4	9.8 \pm 0.6
H ₃ PO ₄ (acid-dry)	253 \pm 8	9.2 \pm 0.5	12.3 \pm 0.9
HClO ₄ (acid-dry)	245 \pm 10	9.1 \pm 0.3	10.6 \pm 1.1

References

- [1] N. Mittal, R. Jansson, M. Widhe, T. Benselfelt, K. M. O. Håkansson, F. Lundell, M. Hedhammar, L. D. Söderberg, *ACS Nano* **2017**, *11*, 5148-5159.
- [2] N. Mittal, F. Ansari, K. Gowda.V, C. Brouzet, P. Chen, P. T. Larsson, S. V. Roth, F. Lundell, L. Wågberg, N. A. Kotov, L. D. Söderberg, *ACS Nano* **2018**, *12*, 6378-6388.
- [3] T. Benselfelt, M. Nordenström, M. M. Hamedi, L. Wågberg, *Nanoscale* **2019**, *11*, 3514-3520.
- [4] A. Buffet, A. Rothkirch, R. Döhrmann, V. Körstgens, M. M. Abul Kashem, J. Perlich, G. Herzog, M. Schwartzkopf, R. Gehrke, P. Müller-Buschbaum, S. V. Roth, *J Synchrotron Radiat.* **2012**, *19*, 647-653.
- [5] T. Benselfelt, J. Engström, L. Wågberg, *Green Chem.* **2018**, *20*, 2558-2570.
- [6] M. Henriksson, L. A. Berglund, P. Isaksson, T. Lindström, T. Nishino, *Biomacromolecules* **2008**, *9*, 1579-1585.
- [7] C. Villagrán, M. Deetlefs, W. R. Pitner, C. Hardacre, *Anal. Chem.* **2004**, *76*, 2118-2123.
- [8] Y. Marcus, A. Loewenschuss, *Annual Reports Section "C"(Physical Chemistry)* **1984**, *81*, 81-135.
- [9] R. B. Adusumali, M. Reifferscheid, H. Weber, T. Roeder, H. Sixta, W. Gindl, *Macromolecular Symposia* **2006**, *244*, 119-125.
- [10] H.-L. Gao, R. Zhao, C. Cui, Y.-B. Zhu, S.-M. Chen, Z. Pan, Y.-F. Meng, S.-M. Wen, C. Liu, H. A. Wu, S. H. Yu, *Natl. Sci. Rev.* **2019**.
- [11] P. Mohammadi, M. S. Toivonen, O. Ikkala, W. Wagermaier, M. B. Linder, *Sci. Rep.* **2017**, *7*, 11860.
- [12] H. Mertaniemi, C. Escobedo-Lucea, A. Sanz-Garcia, C. Gandía, A. Mäkitie, J. Partanen, O. Ikkala, M. Yliperttula, *Biomaterials* **2016**, *82*, 208-220.
- [13] S. Iwamoto, A. Isogai, T. Iwata, *Biomacromolecules* **2011**, *12*, 831-836.
- [14] S. Hooshmand, Y. Aitomäki, N. Norberg, A. P. Mathew, K. Oksman, *ACS Appl. Mater. Interfaces* **2015**, *7*, 13022-13028.
- [15] A. Walther, J. V. I. Timonen, I. Díez, A. Laukkanen, O. Ikkala, *Adv. Mater.* **2011**, *23*, 2924-2928.
- [16] J. G. Torres-Rendon, F. H. Schacher, S. Ifuku, A. Walther, *Biomacromolecules* **2014**, *15*, 2709-2717.
- [17] K. M. O. Håkansson, A. B. Fall, F. Lundell, S. Yu, C. Krywka, S. V. Roth, G. Santoro, M. Kvick, L. Prah Wittberg, L. Wågberg, L. D. Söderberg, *Nat. Commun.* **2014**, *5*, 4018.
- [18] M. J. Lundahl, A. G. Cunha, E. Rojo, A. C. Papageorgiou, L. Rautkari, J. C. Arboleda, O. J. Rojas, *Sci. Rep.* **2016**, *6*, 30695.